

Number of Electrons per Collision as a Quark-Gluon Plasma Signal

C.Dib¹, O.Espinosa¹, P.D.Morley² and I.Schmidt¹

Department of Physics
Universidad Técnica Federico Santa María
Casilla 110-V
Valparaíso, Chile

Abstract

We investigate whether the total number of electrons per collision, as a function of beam energy, is a potential quark-gluon-plasma (QGP) signature. At high beam energies, we find that, after experimental removal of the noise induced by Dalitz decays, the number of produced electrons is increased many times fold from the existence of the QGP. The robustness of the potential signal to differing theoretical assumptions makes it an attractive experimental parameter.

PACS: 25.75.+r, 12.38.Mh, 24.85.+p

¹e-mail: cdib@sutsm.cl or ischmidt@sutsm.cl

²Visitor

Work is in progress to construct a relativistic heavy-ion collider to test the theoretical prediction [1] that QCD (quantum chromodynamics) undergoes a phase transition to unconfined quarks and gluons at high temperatures. Success or failure rides on the identification of an experimental signature which indicates when a QGP has been achieved. The complexities of rhic, however, are such that a QCD description from first principles will be a long range task. Questions of chemical equilibrium, quark effective masses, different flavor and gluon temperatures are just some of the many particulars which have no universal theoretical consensus. Even a parton description is not as adequate for rhic as it is for, say, deeply inelastic scattering, since the nuclear medium modifies the parton distribution functions and interaction amplitudes. Thus from the experimental point of view, a QGP characteristic is desired which is independent of the inclusion of the multitude of indeterminate theoretical minutiae. Original ideas to detect the QGP phase are based on distributions of produced leptons and photons[2], and to date much work is being done to understand the issues involved[3]. However, what we seek here is a robust QGP signal, that will survive the fine details. We demonstrate that the total number of direct electrons per collision as a function of beam energy is just such a signature.

The Result

In Fig. 1 we represent the simulation of the production of electrons in rhic, after the subtraction of Dalitz decays of the low mass hadrons π^0 ; η ; ω ; ρ^0 , i. e. the directly produced electrons. The Dalitz decays constitute the background (noise) from which the signal is to be extracted. While the number of mesons expected per collision numbers in the thousands (see Fig. 2), the accompanying number of directly produced electrons, Fig. 1, can be counted by the fingers of one's hands. Identifying and subtracting the Dalitz electron pair background does not represent severe difficulties.

There are two important physical effects associated with the presence of

a QGP in conjunction with the measurement of the total number of directly produced electrons per collision, as the beam energy is stepped up. When the energy density of the hadron phase first reaches the QGP transition value, allowing a mixture of the hadronic matter to coexist with the QGP, the number of electrons increases more rapidly, with a discernable gradual change in slope around the critical beam energy (10–15 GeV/u; see Fig. 1): this constitutes the first QGP electron signature. Indeed, if one assumes no QGP, from a low beam energy region (say, 5 GeV/u) to a high one (say, 30 GeV/u), the slope of the lepton yield increases by a factor of 30, while if there were a QGP formation at a critical value in between, the slope would increase by a factor of 200. This is 6 times larger than in the previous case. The fact that there is this change in slope is independent of the theoretical uncertainties and is due to the increased degrees of freedom associated with the QGP. Past the onset of the appearance of the QGP, as shown in Fig. 1, the now more rapid electron production rate results in a value for the number of directly produced electrons per collision many times larger than that in a pure hadron gas: this is the second QGP signature. Again, physically, the QGP produces more direct electrons due to the increased number of degrees of freedom. The simplicity in the origin of this signal is at the same time its robustness: no details in the model or uncertainties in the parameters used cannot cause a misleading signal. Indeed, we have varied the values of different parameters of the model over reasonable ranges and found no significant change in the two electron signals. We now discuss how this was simulated.

Derivation of the Result

In central collisions of heavy projectile-target combinations of nuclei, for $E_{\text{lab}} > 1 \text{ GeV/u}$, we expect the formation of thermally equilibrated or nearly equilibrated matter (i. e. a "reball") with subsequent hadronization; for beam energies below 1 GeV/u, no reball should form, since in that

case heavy-ion collisions are adequately described by the participant spectator model, in which individual nucleons collide while the spectator nucleons remain cold and undetected. If E_{lab} is increased, the initial temperature of the reball also increases, and then subsequently drops down as the reball progressively expands. QCD should undergo a first order phase transition at a given temperature T_c . For gluonic matter, lattice gauge theory suggests a transition temperature T_c of about 207 MeV. For the temperature ranges involved, it is sufficient to consider QCD with just two massless quark flavors (u and d). In describing the time evolution of the strongly interacting matter, we take as the equations of motion relativistic hydrodynamics[4].

The picture of a hadronic reball described by 1-D relativistic hydrodynamics, with longitudinal expansion and subsequent pion freeze-out, has been experimentally verified by the CERN SPS central S + S collisions at 200 GeV/c per nucleon [5]. This formulation requires equations of state (EOS), the notion of which implies the existence of an equilibrated initial uniform piece of nuclear matter. Since pionization of nuclear matter occurs already for $T > 50$ MeV, the EOS for hadronic matter in the relevant temperature range is chosen to be that of a (relativistic) pion gas plus a (non-relativistic) nucleon gas. The EOS for hadronic matter (pressure P_{had} vs. energy density ϵ_{had}) is given in parametric form by:

$$P_{\text{had}} = \frac{T^4}{6} \sum_0^Z \int_0^1 dx \frac{x^4}{x^2 + m^2} = \sum_{1,0,1} \frac{1}{e^{(x^2 + m^2)/T}} \quad (1)$$

$$+ \frac{2T^4}{3} \sum_0^Z \int_0^1 dx x^4 = \sum_{p,n} \frac{(2m)^{3/2}}{e^{x^2 + m^2}/T + 1}$$

$$\epsilon_{\text{had}} = \frac{T^4}{2} \sum_0^Z \int_0^1 dx x^2 \frac{x^2}{x^2 + m^2} = \sum_{1,0,1} \frac{1}{e^{(x^2 + m^2)/T}} \quad (2)$$

$$+ \frac{T^4}{2} \sum_0^Z \int_0^1 dx x^2 = \sum_{p,n} \frac{(m^2 + x^2)(2m)^{3/2}}{e^{x^2 + m^2}/T + 1}$$

where we denote $m = T$, $\sim = T$, etc. In each expression, the first sum indicates the contributions from π , 0 and $+$, respectively (we use

the fact that $\bar{q} = q$, since q and \bar{q} are mutually antiparticles, while $\bar{q} = q$ since q is its own antiparticle), and the second sum indicates the contributions from the nucleons (p = proton, n = neutron). For numerical purposes, we found it a good approximation for the EOS of the hadron phase to use $P_{\text{had}} = 0.3 P_{\text{had}}$ in the rhic temperature regime.

For the quark-gluon plasma, the EOS is determined from a non-interacting relativistic gas of massless u and d quarks and gluons, along with the vacuum pressure (B constant), which takes into consideration color confinement as in a Bag model (this parameter is necessary for the phase transition to be of first order). The corresponding EOS is thus described by:

$$P_{\text{QGP}} = \frac{T^4}{2} \int_0^1 dx x^3 \sum_{q=u,d} \left[\frac{1}{e^{x-\mu_q} + 1} + \frac{1}{e^{x+\mu_q} + 1} \right] + \frac{8}{45} T^4 - B \quad (3)$$

$$P_{\text{QGP}} = \frac{3T^4}{2} \int_0^1 dx x^3 \sum_{q=u,d} \left[\frac{1}{e^{x-\mu_q} + 1} + \frac{1}{e^{x+\mu_q} + 1} \right] + \frac{8}{15} T^4 + B \quad (4)$$

where $\mu_q = qT$, for $q = u, d$. The first and second terms in the sum are the contributions from q and \bar{q} , respectively, while the last two terms are the contributions from the gluons and the (deconfined) vacuum, respectively. In the case of zero chemical potentials (zero net baryon number and electric charge), Eqs. (3) and (4) assume the simple form :

$$P_{\text{QGP}} = \frac{37}{3} \left(\frac{T}{30} \right)^4 - B \quad (5)$$

$$P_{\text{QGP}} = 37 \left(\frac{T}{30} \right)^4 + B : \quad (6)$$

which, for $T_c = 207 \text{ MeV}$ give $B^{1/4} = 288 \text{ MeV}$.

In the general case of a net baryon number and/or net electric charge present, the equilibrium between the two phases is determined by the three equations in the three unknowns T_c ; μ_c ; μ_B (critical temperature, electric charge chemical potential, baryonic number chemical potential):

$$\begin{aligned} P_{\text{had}}(\mu_q; \mu_p; \mu_n; T_c) &= P_{\text{QGP}}(\mu_u; \mu_d; T_c) \\ Q &= N_p + N_{\bar{p}} + N_{\bar{n}} + \frac{2}{3}(N_u - N_{\bar{u}}) - \frac{1}{3}(N_d - N_{\bar{d}}) \\ B &= N_p + N_n + \frac{1}{3}(N_u - N_{\bar{u}}) + \frac{1}{3}(N_d - N_{\bar{d}}) \end{aligned} \quad (7)$$

where $Q, B, N_p, N_n, N_u, N_{\bar{u}}, \dots$, etc are the respective electric charge, baryon number, proton, neutron, u-quark, anti-u-quark, ..., etc number densities. The electric charge and baryon number, Q and B , are input parameters and at the same time the two conserved quantities in the thermal problem, so there are only two independent chemical potentials, namely μ_c and μ_B , in terms of which we can express those for each species:

$$\begin{aligned}
 \mu_{\pi^+} (= \mu_{\pi^-}) &= \mu_c \\
 \mu_p &= \mu_c + \mu_B \\
 \mu_n &= \mu_B \\
 \mu_u (= \mu_{\bar{u}}) &= \frac{2}{3} \mu_c + \frac{1}{3} \mu_B \\
 \mu_d (= \mu_{\bar{d}}) &= \frac{1}{3} \mu_c + \frac{1}{3} \mu_B
 \end{aligned} \tag{8}$$

In the simultaneous solution of these equations, we find that the effect of a net baryon number on the value of T_c is negligible, for the densities used in the rhic simulation. Thus the important energy densities, which are shown in Table 1, are fixed by the temperature alone.

As the collision energy is increased, the first appearance of the QGP occurs when the energy density reaches $\epsilon_{had}^{(c)}$ ($0.22 \text{ GeV}/\text{fm}^3$), at $T_c = 207 \text{ MeV}$. Because the phase transition is modeled to be first order, a latent energy density, $4B$, must then be supplied in order to liberate the quarks and reach a 100 % QGP. This happens when the energy density reaches $\epsilon_{QGP}^{(c)}$ ($3.81 \text{ GeV}/\text{fm}^3$). If the initial energy density, ϵ_i , is between 0.22 and $3.81 \text{ GeV}/\text{fm}^3$, the matter is in a mixture of the two phases, in which the initial proportion of QGP present, f_i , satisfies $\epsilon_i = \epsilon_{QGP}^{(c)} f_i + \epsilon_{had}^{(c)} (1 - f_i)$.

Two parameters describe the collision previous to thermalization: the compression factor, β , and the stopping power, S . The volume V_{fb} of the initial reball is taken to be the sum of the volumes of the individual nuclei divided by the compression factor:

$$V_{fb} = v_n (A_1 + A_2) = ; \quad v_n \approx 7.2 \text{ fm}^3/\text{nucleon}; \tag{9}$$

where v_n is the nuclear specific volume, and A_1 and A_2 are the mass numbers of the colliding nuclei. The old idea that the reball can be infinitesimally small, based on the fact that the colliding nuclei are Lorentz contracted ‘pancakes’, is rejected; modern computations disclose that a finite time interval is required for equilibration and the compression factor reaches a quasi-constant value of the order of 4.0 at the highest energies[6]. Thus we have adopted a sliding value of β from 1 to 4. The other major parameter is the stopping power, S , i.e. the average fraction of CM S kinetic energy a nucleon loses in the collision. For identical nuclei of baryon number A , the CM S thermal energy available for hydrodynamic expansion is

$$E_T = 2A (E_N - m_N) S; \quad (10)$$

where E_N is the CM S incident energy per nucleon and m_N the nucleon mass. Experimentally, $S \approx 0.7$ only at high energies, while modest for small energies. Thus we also made S a sliding linear function of E_N . These two parameters are set by the CERN SPS S + S rhic data [5] to be about $S \approx 0.5$ and $\beta \approx 1.4$ for incident CM S energy per nucleon $E_N = 9.7$ GeV.

The last consideration is the choice of the relativistic hydrodynamic description. Event shapes at high energy are not isotropic, but rather elongated along the beam axis[5] so we choose a 1-D longitudinal simulation. A phenomenological parton Monte-Carlo simulation [7] gave results remarkably resembling those of a 1-D longitudinal hydrodynamic flow [4].

Full numerical solutions including the EOS (1)–(4) and phase coexistence conditions (7)–(8) were studied. As mentioned above, effects of net baryon charge were found not to be significant, in which case the approximate EOS $P_{\text{had}} = \beta_{\text{had}} \epsilon_{\text{had}}$ for hadrons and for Eqs. (5)–(6) for QGP matter allow an analytical solution to the 1-D hydro flow: let $\tau = \sqrt{t^2 - z^2}$ be the proper time of a given fluid element (t, z being the spacetime coordinates from the origin of collision in the CM S); using $\tau_0 = 1$ Fermi/c as the initial time (i.e. the estimated time for formation and equilibration of the reball), for a high initial temperature the fluid element will start as QGP, cool down as

it expands reaching T_c at $\tau = \tau_1$, condense to a full hadronic phase at $\tau = \tau_2$ and subsequently cool below T_c until freeze out. The temperature T and energy density ϵ in the QGP, mixed and hadronic phases, respectively, are given by:

$$\begin{aligned} \text{QGP : } T(\tau) &= T(\tau_0) = (\epsilon_0 = \epsilon_0^{\text{QGP}})^{1/3}; \quad (\epsilon(\tau) - \epsilon_B) = (\epsilon_0 - \epsilon_B) = (\epsilon_0^{\text{QGP}} - \epsilon_B)^{4/3} \\ \text{mixed : } T(\tau) &= T_c; \quad \epsilon(\tau) = \epsilon_{\text{QGP}} f(\tau) + \epsilon_{\text{had}} (1 - f(\tau)) \quad (11) \\ \text{hadronic : } T(\tau) &= T(\tau_2) = (\epsilon_2 = \epsilon_2^{\text{had}})^{1/3}; \quad \epsilon_{\text{had}}(\tau) = \epsilon_{\text{had}}(\tau_2) = (\epsilon_2^{\text{had}})^{4/3} \end{aligned}$$

where $f(\tau) = 1 - [1 - f(\tau_1)] s_{\text{QGP}} / (s_{\text{QGP}} - s_{\text{had}})$ is the fraction of QGP in the mixed phase, s being the entropy density $s = (\epsilon + P)/T$.

The simulation now proceeds as follows: at each beam energy, the initial energy density and temperature are calculated. Determination is made if the strongly interacting matter is in the hadronic phase (pions), mixed phase, or pure QGP phase. An estimate of the prompt electrons is then done, by computing the dilepton rate for one time step (units in Fermi/c) over the initial reball volume of a pion gas (the prompt electrons come from the initial reball formation and do not know the existence of any subsequent QGP). After this, the hydro-expansion begins: the edges are advanced one time unit using the hydro-solution and the fluid is divided into zones. The new temperature is recomputed for the middle of each zone and the appropriate dilepton rate determined, taking into account that the zone may be in a new phase. The electron rate in the QGP is due to quark-quark and quark-gluon collisions [8] (Fig. 3) and in the hadronic phase is due to pion annihilation [9] and virtual bremsstrahlung from pion scattering [10]. Here we did not include heavier mesons [11] in our analysis, so that we may be slightly underestimating the lepton yield from the hypothetical hadronic reball at high temperatures (i.e. above 1 GeV, that is, well above T_c). Also, finite temperature and density effects were not included, since they are small corrections [12] to the pion annihilation amplitude in vacuum. Those zones which have an energy density less than half-nuclear experience freeze-out and do not produce any more particles (electrons and mesons). The approximate freeze-out temperature

is 154 MeV, with the approximate pion number density 135 fm^{-3} . By integrating over the invariant mass of the lepton pairs and then summing each zone contribution, the total production of electrons is ascertained for that time interval. We consider a reball with mirror symmetry around $z = 0$ and cylindrical symmetry about the beam axis. The time counter is advanced an additional Fermi/c and the hydro-expansion continues until all zones experience freeze-out. The result, Fig. 1, for the number of produced electrons as a function of the beam energy is obtained. As mentioned earlier, the 1-D hydrodynamic model works very well with the CERN SPS S+ S meson data, which constrains the model parameters α and S . For those values, Fig. 2 shows the pion yield, corresponding to the number of pions in the reball at the moment of freeze-out.

There is a distinctive increase in the number of directly produced electrons, once the beam energy becomes high enough for the QGP phase to form. The physical reason for this manifold increase of directly produced electrons due to the existence of the QGP is the increased number of degrees of freedom. This signal is independent of the particulars of the rhic simulation. Indeed, for the broad range of values of the phenomenological parameters considered, namely the stopping power S , the compression factor α and the effective gluon mass, the resulting direct electron signal showed no appreciable change. Thus, one might also expect an increased number of hard photons, although the analysis of that signal was not considered in this work.

Acknowledgements

One of us (P.D.M.) is grateful to L. Ray of the STAR detector at RHIC for useful discussions. This work was supported in part by FONDECYT (Chile), contracts 1950685 and 1960536.

References

- [1] J. W. Harris and B. Muller, Duke Univ. preprint DUKE-TH-96-105, Feb. 1996, hep-ph/9602235, submitted for publication to Ann. Rev. of Nucl. and Part. Science, and references therein.
- [2] E. Feinberg, Nuovo Cimento A 34 (1976) 39; E. V. Shuryak, Phys. Lett. 79B (1978) 135.
- [3] See e.g. J. Steele, H. Yamagishi, I. Zahed, Phys. Lett. 384B (1996) 255; C. M. Hung, E. V. Shuryak, SUNY preprint SUNY-NTG-96-16, hep-ph 9608299, and references therein.
- [4] L. D. Landau, Collected Papers (Pergamon, NY, 1965) 569; J. D. Bjorken, Phys. Rev. D 27 (1983) 140; K. Kajantie et al., Phys. Rev. D 34 (1986) 2746; Cheuk-Yin Wong, Introduction to High-energy Heavy-ion Collisions (World Scientific Press, Singapore, 1994).
- [5] J. Bachler et al. (NA 35 Collaboration), Phys. Rev. Lett. 72 (1994) 1419.
- [6] R. Anishetty, P. Koehler and L. McLerran, Phys. Rev. 22 (1980) 2793.
- [7] K. Geiger, Phys. Reports 258 (1995) 334.
- [8] R. D. Field, Applications of Perturbative QCD, Frontiers in Physics, Addison-Wesley Pub. Co., 1989; K. Geiger and J. Kapusta, Phys. Rev. Lett. 70 (1993) 1920; for QCD and thermal corrections: J. Cleymans, I. Dadić and J. Joubert, Phys. Rev. D 49 (1994) 230.
- [9] G. Domokos and J. I. Goldmann, Phys. Rev. 23 (1981) 203; C. Gale and P. Lichard, Phys. Rev. D 49 (1994) 3338.
- [10] K. Haglin et al., Phys. Rev. D 47 (1993) 973.
- [11] C. Song, C. M. Ko, C. Gale, Phys. Rev. D 50 (1994) 1827R.
- [12] C. Gale and J. I. Kapusta, Nucl. Phys. B 357 (1991) 65; C. Song, V. Koch, S. H. Lee, C. M. Ko, Phys. Lett. 366B (1996) 379.

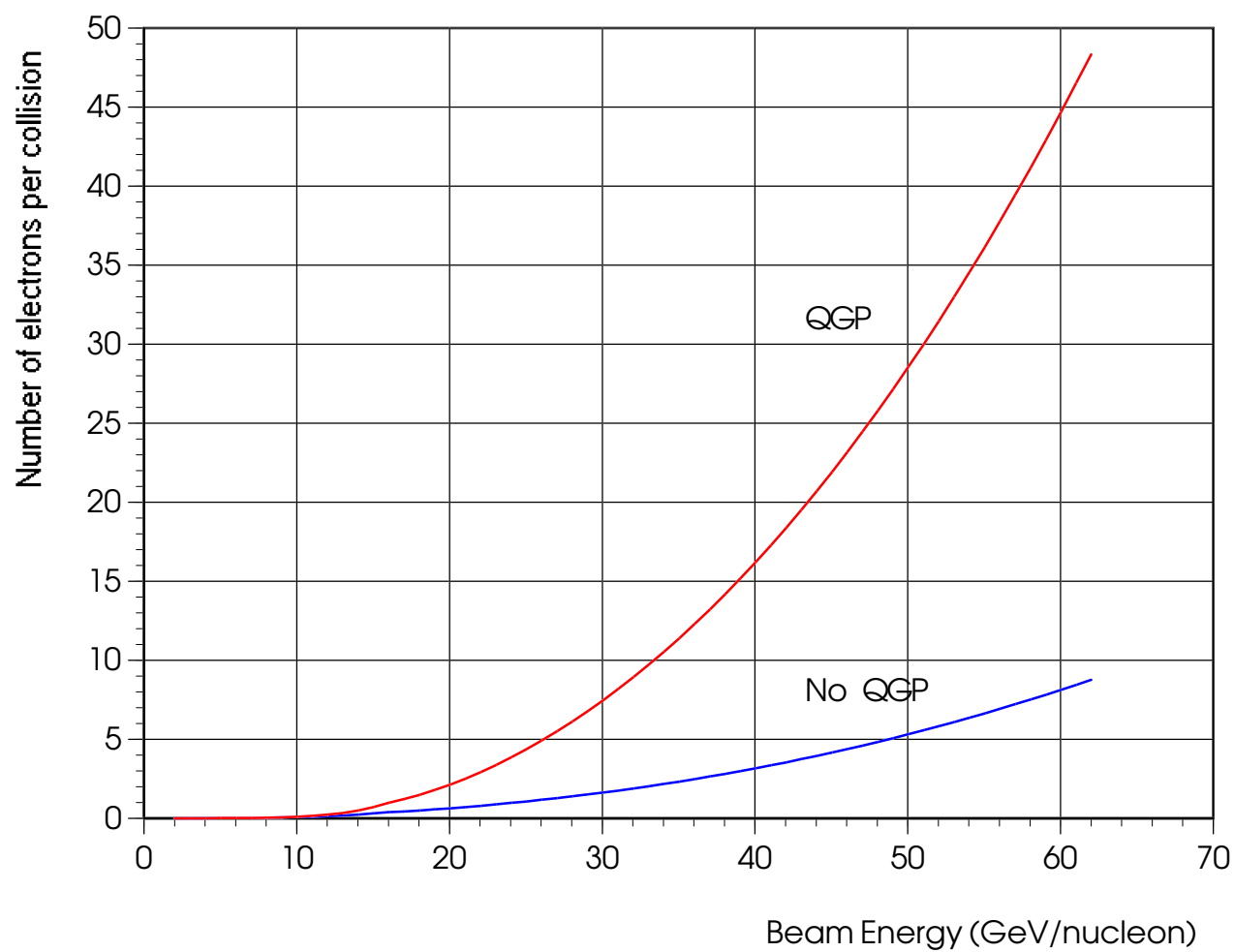
Figure Captions

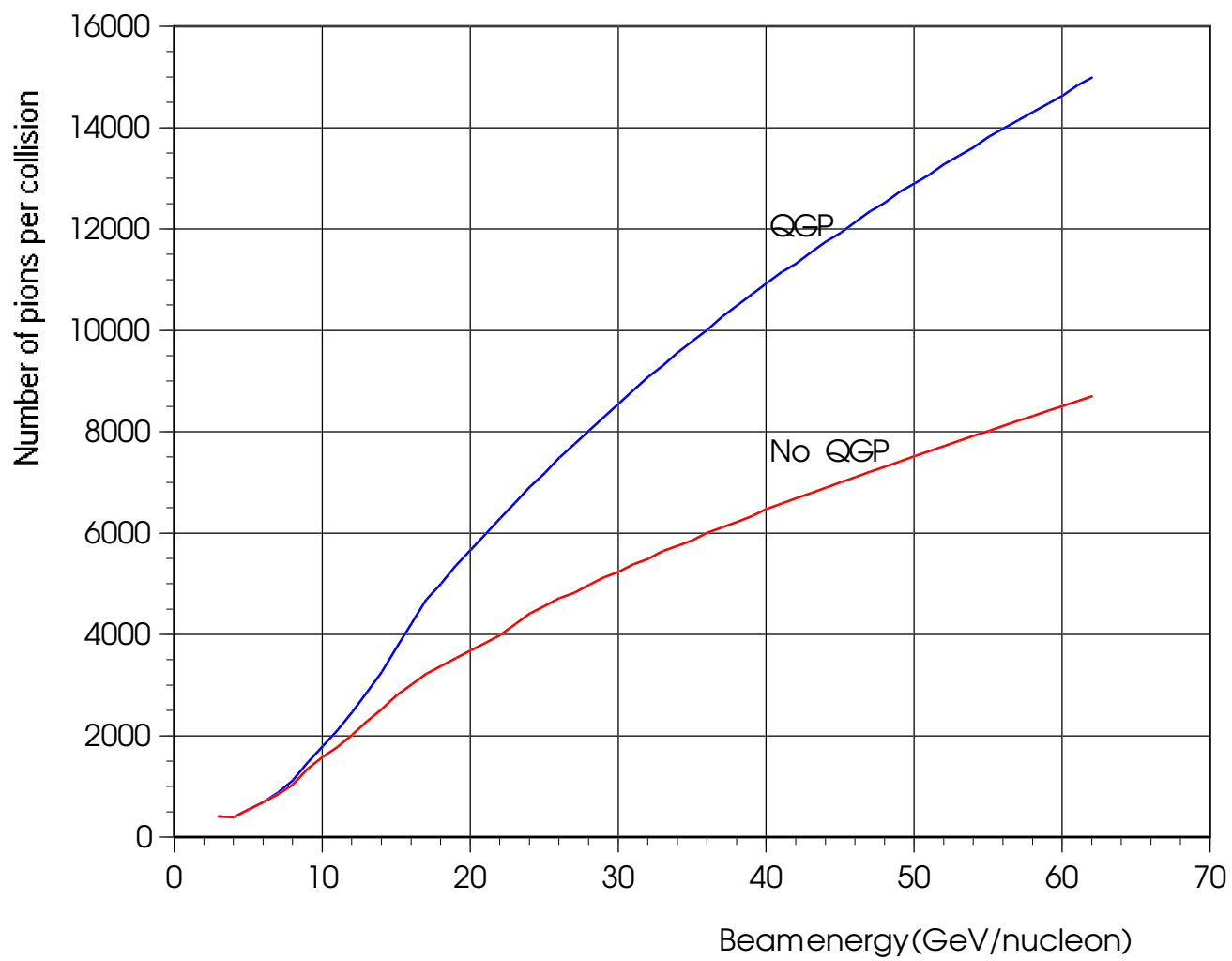
1. The number of electrons per collision versus beam energy (GeV per nucleon), for Au vs. Au, after subtraction of the Dalitz noise. The CM S energy is twice the beam energy, for identical nuclei.
2. The number of pions per collision versus beam energy (GeV per nucleon), for Au vs. Au. The CM S energy is twice the beam energy, for identical nuclei.
3. The processes contributing to the production of dielectrons in the quark-gluon plasma.

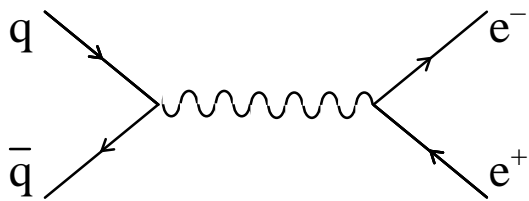
Table

| | |
|--|--------------------------|
| e^+e^- freeze-out (half nuclear energy density) | 0.065 GeV/fm^3 |
| nuclear energy density | 0.13 GeV/fm^3 |
| hadron energy density at the phase transition: $\epsilon_{\text{had}}^{(c)}$ | 0.22 GeV/fm^3 |
| QGP energy density at the phase transition: $\epsilon_{\text{QGP}}^{(c)}$ | 3.81 GeV/fm^3 |

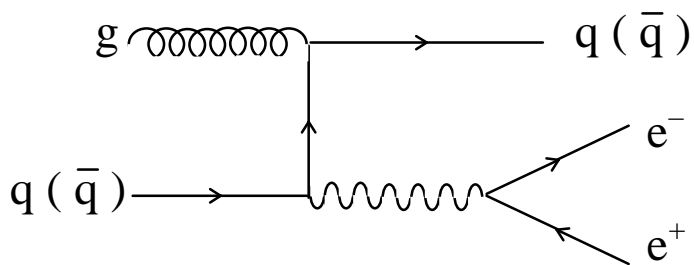
Table 1: Relevant energy densities in rhic.



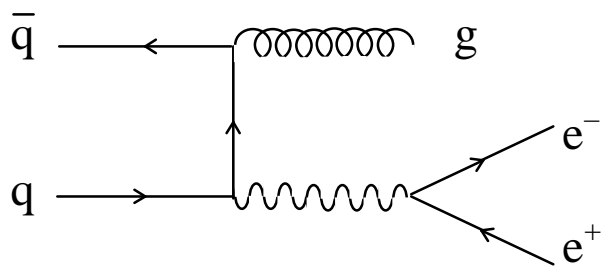




(a)



(b)



(c)

